

Controlling the growth of Bi(110) and Bi(111) films on an insulating substrate

This content has been downloaded from IOPscience. Please scroll down to see the full text.

2017 Nanotechnology 28 155602

(<http://iopscience.iop.org/0957-4484/28/15/155602>)

View [the table of contents for this issue](#), or go to the [journal homepage](#) for more

Download details:

IP Address: 130.89.45.232

This content was downloaded on 25/04/2017 at 10:33

Please note that [terms and conditions apply](#).

You may also be interested in:

[Orientationally textured thin films of W₂O₃ deposited by pulsed laser deposition](#)

A J Caruana and M D Cropper

[Influence of Film Roughness on the Soft Magnetic Properties of Fe/Ni Multilayers](#)

Luo Zhi-Yuan, Tang Jia, Ma Bin et al.

[Structure and stability of Pr₂O₃/Si\(0 0 1\) heterostructures grown by MBE using a high temperature effusion source](#)

B P Tinkham, M Takahasi, B Jenichen et al.

[Ultrathin Bi films on Si\(100\)](#)

C Bobisch, A Bannani, M Matena et al.

[Growth morphology of thin films on metallic and oxide surfaces](#)

Aleksander Krupski

[Stress evolution during growth of GaN \(0001\)/Al₂O₃\(0001\) by reactive dc magnetron sputter epitaxy](#)

M Junaid, P Sandström, J Palisaitis et al.

[Study of Dy-doped Bi₂Te₃: thin film growth and magnetic properties](#)

S E Harrison, L J Collins-McIntyre, S-L Zhang et al.

[Strain driven monoclinic distortion of ultrathin CoO films in the exchange-coupled CoO/FePt/Pt\(001\) system](#)

Anne D Lamirand, Márcio M Soares, Maurizio De Santis et al.

[Thin film growth studies using time-resolved x-ray scattering](#)

Stefan Kowarik

Controlling the growth of Bi(110) and Bi(111) films on an insulating substrate

Maciej Jankowski¹, Daniel Kamiński², Kurt Vergeer³, Marta Mirolo¹,
Francesco Carla¹, Guus Rijnders³ and Tjeerd R J Bollmann^{3,4}

¹ESRF-The European Synchrotron, 71 Avenue des Martyrs, F-38000 Grenoble, France

²Department of Chemistry, University of Life Sciences in Lublin, 20-950, Poland

³University of Twente, Inorganic Materials Science, MESA+ Institute for Nanotechnology, PO Box 217, NL-7500AE Enschede, The Netherlands

E-mail: t.r.j.bollmann@utwente.nl

Received 1 December 2016, revised 1 February 2017

Accepted for publication 21 February 2017

Published 16 March 2017



CrossMark

Abstract

We demonstrate the controlled growth of Bi(110) and Bi(111) films on an α -Al₂O₃(0001) substrate by surface x-ray diffraction and x-ray reflectivity using synchrotron radiation. At temperatures as low as 40 K, unanticipated pseudo-cubic Bi(110) films are grown with thicknesses ranging from a few to tens of nanometers. The roughness at the film–vacuum as well as the film–substrate interface, can be reduced by mild heating, where a crystallographic orientation transition of Bi(110) towards Bi(111) is observed at 400 K. From 450 K onwards high quality ultrasmooth Bi(111) films form. Growth around the transition temperature results in the growth of competing Bi(110) and Bi(111) domains.

Supplementary material for this article is available [online](#)

Keywords: bismuth, sapphire, surface x-ray diffraction

(Some figures may appear in colour only in the online journal)

1. Introduction

Nanostructured ultrathin Bi films have recently attracted a lot of interest as they reveal exotic magneto-electronic properties making them appealing materials for spintronic applications [1–12]. Especially the spin-momentum locked surface states of topological insulating Bi films [13–16], make them very attractive candidates for spintronic devices. To develop and optimize topological insulators (TIs) towards applications, thin films of high quality are a necessity, as otherwise the exotic electronic properties are hampered by bulk conduction [7, 17, 18]. To minimize the contribution of the substrate [10], an atomically well defined insulating substrate, providing an infinite potential well barrier, is essential for both future electronic applications as well as to get a deeper understanding on the controllability of Bi growth. This choice of substrate is also very beneficial for practical applications, as the interface will be protected from oxidation effects from

ambient exposure. It is this interface between the film and insulating oxide which is expected to reveal topological states [19]. Although a direct dry transfer of a single-crystalline thin film onto arbitrary substrates as recently demonstrated may be a viable route towards applications [20], the resulting thin film quality and its properties at the interface is rather hard to control upon transfer. The direct growth onto a suitable substrate should be preferred as it leads to a well defined interface and highest possible film quality. The growth of Bi has been extensively studied on Si(111) [21–30] and highly oriented pyrolytic graphite [13, 31–33] as well as other surfaces [3, 4, 12, 34–40], resulting in fabrication of films with a range of different morphologies, orientations, and strain. The fabrication of Bi films has attracted considerable interest in recent years, as their controlled growth, with focus on morphology and crystallographic orientation, on semiconductor and oxide surfaces is not a trivial task. It is well-known that metals on semiconductors and oxides usually show 3D growth modes [41] instead of atomically smooth (2D) films. However, this problem can be overcome by use of

⁴ Author to whom any correspondence should be addressed.

deposition at low temperatures [42, 43] or surfactant-mediated growth [44, 45], as it modifies the film kinetics.

In this study we demonstrate by surface x-ray diffraction (SXRD) the controlled growth of thin Bi(110) and Bi(111) films (the index used throughout this paper refers to the rhombohedral system) on such an insulating substrate: atomically smooth insulating sapphire (α -Al₂O₃(0001)) having a lattice mismatch of 4.6% with Bi(111), so large that thermal mismatch might be ignored. The preparation of pseudo-cubic (110)-oriented Bi films, a rather exotic orientation, is a difficult task [46]. At temperatures as low as 40 K, we are able to slow down kinetics resulting in a high nucleation density of Bi islands and thereby controlling the growth of Bi towards smooth Bi(110) films, stable up to 400 K. By annealing the Bi(110) films beyond this temperature, they can be transformed towards stable Bi(111) films. For films grown around RT, a competition between (110) and (111) thin film domains is observed.

2. Experimental

For the SXRD experiments described here, we used hat shaped α -Al₂O₃(0001) single crystals with a miscut of $<0.2^\circ$. Prior to annealing for 12 h in a tube furnace at 1323 K using an O₂ flow of 150 l h⁻¹, the samples have been ultrasonically degreased in acetone and ethanol. The samples were then initially inspected by tapping mode atomic force microscopy (TM-AFM) for their stepheight (0.21 nm between two adjacent oxygen planes) and terrace width (\sim 300 nm), and x-ray photoelectron spectroscopy to verify the surface cleanliness where only minor traces of C and Ca were found, see supplementary material available online at stacks.iop.org/NANO/28/155602/mmedia. After insertion into the UHV system of the surface diffraction beamline ID03/ESRF (Grenoble, France) [47] with a base pressure below 1×10^{-10} mbar, the sample was cleaned by mild 700 eV Ar⁺ sputtering at $p(\text{Ar}) = 3 \times 10^{-6}$ mbar and subsequent annealing to 1200 K in an O₂ background pressure of 1×10^{-6} mbar cycles, where we monitored the sample quality by Auger electron spectroscopy, see supplementary material. Bi was deposited at a typical deposition rate of 1.3 Å per minute from a Mo crucible mounted inside an electron-beam evaporator (Omicron EFM-3). According to the bulk phase diagram, Bi and sapphire are immiscible in the bulk [48]. The SXRD experiments were performed using a monochromatic synchrotron x-ray beam at 24 keV and a MAXIPIX detector [49] with 512×512 pixels. For data integration and the creation of reciprocal space maps from the 2D detector frames we used the BINoculars software package [50]. All reciprocal space positions are given in (h, k, l) measured in reciprocal lattice units of the hexagonal substrate (0001) surface lattice. Bragg peaks of the thin Bi films are labeled by their conventional rhombohedral Miller indices [1]. X-ray reflectivity (XRR) curves have been fitted using the GenX software package [51].

3. Results

In order to determine the surface structure and morphology of the thin Bi films grown *in situ*, we make use of XRR scans, crystal truncation rod (CTR) scans and reciprocal space maps determined by SXRD. The out-of-plane (electronic) density profile measured by XRR provides information on film layer density, film thickness and interface roughness. The measured (00) CTR provides information on the out-of-plane crystallographic orientation of the film. To be sensitive to the in-plane registry we record reciprocal spacemaps (at constant $L = 0.5$). In figures 1(a)–(b) and (c)–(d) we show the (00) CTRs and reciprocal space maps of thin Bi films grown on the sapphire substrate. A sharp pronounced (0006) Bragg peak in (a) and (b) corresponds to the out-of-plane interlayer distance of the sapphire (0001) surface unit cell. Upon growth of a 20 nm thick film at 40 K, a Bragg-peak is found at $L = 4$ corresponding to the 3.25 Å interlayer distance of Bi(110) [1], see figure 1(a). In the reciprocal space map, see figure 1(c), rings appear caused by the rotationally disorder of the Bi(110) domains. The position of the rings perfectly matches to the (011), (112) and ($\bar{1}$ 1 0) Bi planes expected for the Bi(110) surface, as depicted in figure 1(e), and corresponding to in-plane distances of 3.28 Å, 4.75 Å and 4.55 Å respectively. The homogeneously distributed intensity in the rings in figure 1(c), reveal no preferential alignment with respect to the substrate.

Annealing the as grown film up to 400 K, results in the repositioning of the Bi Bragg peak in the recorded (00) CTR to $L = 3.3$, corresponding to the interlayer distance of 3.94 Å for Bi(111) [1], see figure 1(b). The corresponding reciprocal space map is shown in figure 1(d). For this film, also ring structures in the diffracted intensity appear, with the most intense ring position matching the (0 $\bar{1}$ 1) plane, see figure 1(f), and corresponding to an in-plane distance of 4.55 Å. Analogously to the Bi(110) film, the presence of the rings results from rotational disordered Bi(111) domains on the surface. The Bi(111) domains show slight preferential alignment with respect to the six-fold symmetric substrate as can be seen from the increased intensity on the ring close to the (11) CTR, see figure 1(d).

To test both the Bi(110) and Bi(111) film for their thermal stability and to investigate the effects of kinetics on the film roughness, we deposited 14 nm of Bi on the sapphire surface at 40 K and gradually increased the temperature. Figure 2(a) shows XRR curves, revealing the effect of increasing the temperature. At higher temperature, the number of Kiessig fringes and their amplitude, arising from the constructive interference between the x-rays reflected from the film–vacuum and substrate–film interface, increases, indicating the decrease in roughness on both interfaces. At 400 K, the Kiessig fringes are also visible beyond $L = 1.3$. The film consists at this temperature of Bi(110) and Bi(111) domains, discussed below. The reason for the Bi(110) films not transforming below 400 K are the slowed kinetics [41]. When heating the same film beyond 400 K, the film shows a pure Bi(111) crystal structure. For temperatures at 500 K and above (but below the film melting temperature of \sim 545 K

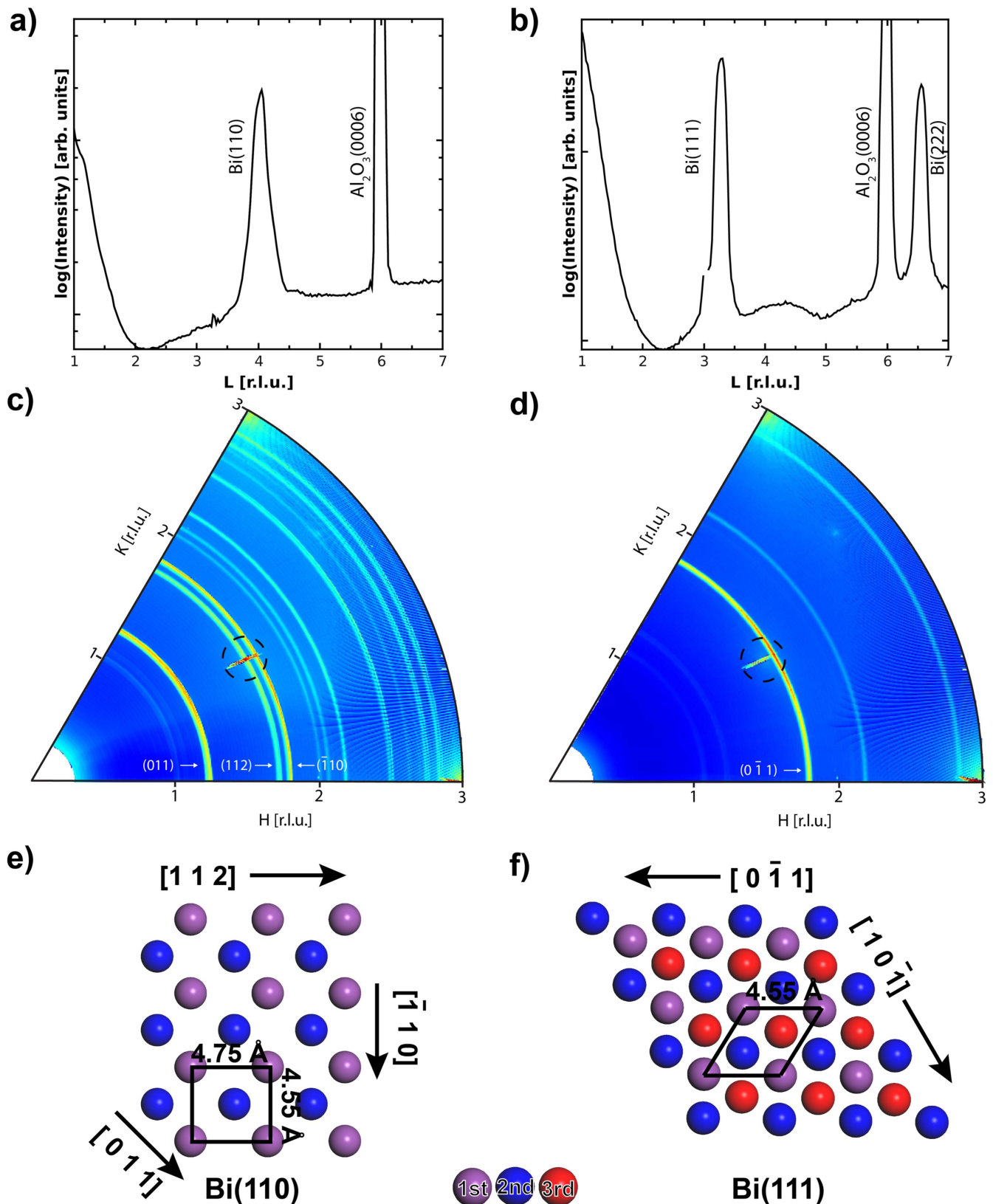


Figure 1. (00) CTR scan for a 20 nm thick Bi(110) film deposited at 40 K revealing the Bi(110) Bragg peak at $L = 4$ (a) and a 20 nm thick Bi(111) film revealing the Bi(111) Bragg peak at $L = 3.3$ after annealing to 400 K (b). The corresponding reciprocal space maps for the 20 nm thick Bi(110) measured at $L = 0.5$ at RT (c) and for the annealed Bi(111) (d) film. The substrate (11) CTR is marked by dashed circles. Next to the diffraction rings, resulting from the rotationally disordered domains, the corresponding miller indices of their crystallographic planes are denoted. (e) A ball model of the pseudo-cubic Bi(110) surface. (f) A ball model of the hexagonal Bi(111) surface. Atoms in the 1st, 2nd and 3rd layer are marked by purple, blue and red colors, respectively.

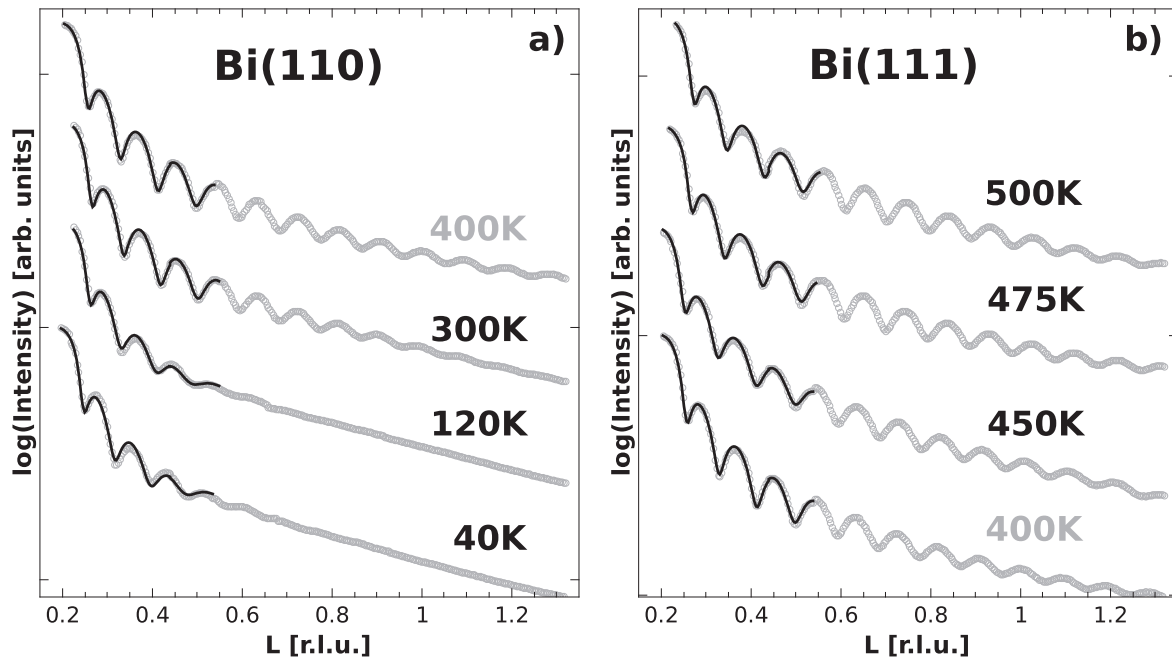


Figure 2. (a) XRR scan for a 14 nm thick Bi(110) film grown at 40 K, heated to and subsequently measured at 120, 300 and 400 K. At 400 K, reflectivity scans reveal a Bi(110) and Bi(111) peak, indicating the crystallographic orientation transition (see also figure 3(a)). (b) XRR scans for the resulting 14 nm thick Bi(111) film heated to and subsequently measured at 450, 475 and 500 K. The solid curves in (a) and (b) have been obtained by fitting as described in the text.

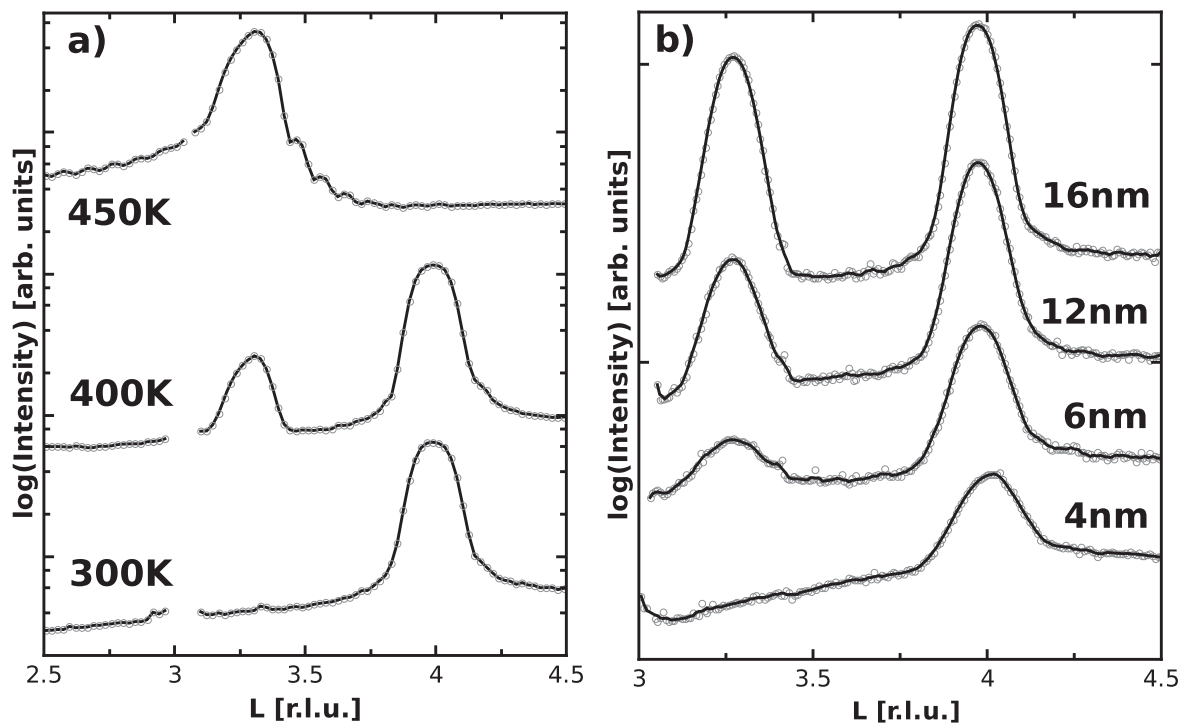


Figure 3. (a) XRR curves for a 14 nm Bi(110) film grown at 40 K (corresponding to figure 2(a)) measured at 300, 400 and 450 K. At 400 K, the onset of the crystallographic orientation transition towards a Bi(111) film is seen where at 450 K the entire film is transformed. (b) XRR curves for increasing Bi film thickness, grown at RT. The first 4 nm, Bi(110) domains are grown, followed by Bi(111) domains starting around 6 nm total Bi film thickness.

depending on film thickness [53]) the number of Kiessig fringes increase even beyond the film Bragg peak at $L = 3.3$, see also figure 3(a).

In order to quantify the roughness for the film–vacuum and substrate–film interface, we model the system as a film of uniform (electronic) density on top of a uniform (electronic) dense substrate. Fitting was done by using the fitting

Table 1. Obtained roughness for the film–vacuum interface ($R_{\text{rms}}^{\text{film}}$), the substrate–film interface ($R_{\text{rms}}^{\text{substrate}}$) and the film thickness (d) from fitting [51] the experimental data as shown in figures 2(a)–(b). The average domain size D is calculated from the Bi(110) and Bi(111) peak broadening [52]. For temperatures < 400 K, the film grown at 40 K is pure Bi(110), for temperatures above pure Bi(111).

$T(\text{K})$	Bi film structure	$R_{\text{rms}}^{\text{film}}(\text{\AA})$	$R_{\text{rms}}^{\text{substrate}}(\text{\AA})$	$d(\text{\AA})$	$D(\text{\AA})$
40	(110)	7.2	8.1	142	80
120	(110)	5.5	9.1	143	80
300	(110)	4.4	3.3	140	80
400	(110) and (111)	4.8	3.2	138	—
450	(111)	< 1	5.7	136	95
475	(111)	< 1	3.2	137	95
500	(111)	< 1	2.6	137	95

parameters film thickness (d), film–vacuum interface roughness ($R_{\text{rms}}^{\text{film}}$), substrate–film interface roughness ($R_{\text{rms}}^{\text{substrate}}$) (see table 1), a background resulting from scattering and a normalization factor [51]. Note that we fit up to limited L (here 0.6) to ensure the dynamical scattering theory is applicable and stay far from the kinetical scattering regime [54].

The roughness for the Bi(110) film–vacuum interface can be reduced by about 40% to 4.4 Å by heating the sample to RT, see table 1. The $R_{\text{rms}}^{\text{substrate}}$ can also be greatly reduced, which may be indicative of the rough initial growth due to the lattice mismatch described above, resulting in an electronic gradient in the profile going from substrate to film. Upon heating, these lattice defects might be restored and the film might be (more) decoupled from its substrate as the roughness for the Bi(110) film at RT is similar to Bi(111) films. The ultrasmooth Bi(111) films, having a $R_{\text{rms}}^{\text{film}}$ below 1 Å, also reveal a decreasing $R_{\text{rms}}^{\text{substrate}}$ upon increasing temperature. Note, that the used modeling only includes a fixed and homogeneous electronic density value for vacuum, film and substrate, giving a very reasonable fit as shown by the solid curves in figures 2(a) and (b). This means that the electronic density profile is close to a step function, indicating the decoupling of electronic density between substrate and film.

By measuring the broadening of the Bi(110) and Bi(111) peak and applying the Scherrer formula [52], we estimate the mean domain size D , see table 1. As the Bi(110) and Bi(111) peaks hardly broaden upon heating, we conclude the mean domain size to stay constant upon heating. Note that the Scherrer formula provides a lower bound on the domain size.

A striking feature in the growth of Bi on sapphire is the appearance of the Kiessig fringes when the film is deposited at 40 K, in contrast to films deposited at RT and above. We expect this to result from 2D island growth as described by Campbell for the growth of metals on oxide surfaces [41]. According to this model, due to the low temperature, the kinetic limitations cause a high nucleation density resulting initially in 2D island growth. Subsequently, the deposited material grows on top of these islands in a layer-by-layer fashion, as between the islands the filling proceeds rather slowly. In literature, there are multiple examples of such growth reported [42, 43, 55, 56], e.g., continuous Ag films on ZnO(0001) are demonstrated to grow at reduced temperature

[57]. For the initial low temperature growth of Bi on quasi-crystal surfaces, small 2D island formation is reported, transforming towards continuous films at higher coverages [39].

Bi(110) films grown at low temperatures can be transformed to ultrasmooth Bi(111) films upon annealing to 450 K. However, interesting is the region in between, as the film shows a crystallographic orientation transition from Bi(110) towards Bi(111) in a temperature window of 300–450 K, see figure 3(a). The 14 nm Bi film shown in figure 3(a) is grown at 40 K and shows only the Bi(110) Bragg peak, heating it to 400 K reveals the onset of a Bi(111) Bragg peak. At a temperature of 450 K the entire film has transformed into an ultrasmooth Bi(111) film as the Bi(110) Bragg peak has vanished. The thin film roughness has been reduced (to a $R_{\text{rms}}^{\text{film}} < 1$ Å) as can be seen from the Kiessig fringes appearing around the Bi(111) Bragg peak at $L = 3.3$. We anticipate this crystallographic orientation transition to be resulting from enhanced kinetics due to surface pre-melting of the thin Bi film [23]. For flat ultrathin Bi(111) films on Si(111)- 7×7 surface pre-melting occurs at about 350 K [23], very similar to our observations. From this data, it is however not evident how the crystallographic orientation transition proceeds. One interpretation could be that at 400 K both Bi(110) and Bi(111) domains are in competition. A more unlikely interpretation could be that a Bi(111) film could be stacked on top of the initially grown Bi(110) film, which would be energetically highly unfavorable. The crystallographic orientation transition of Bi(110) to Bi(111) at a critical film thickness is subject to ongoing debate in literature. According to Nagao *et al* [24, 27], at low film thickness the (puckered-layer) Bi(110) is more stable as a result of surface effects. As the thickness approaches a critical few layers, the surface effects become less dominant, transforming the film to Bi(111), as it becomes energetically more favorable. Similar observations were done by Bobaru *et al* [39] reporting the coexistence of the Bi(110) and Bi(111) domains grown at low temperatures and coverage, as well as the transformation of Bi(110) to Bi(111) domains at higher coverages. There, the coexistence of both crystallographic orientations was attributed to the minor difference in surface free energy of ultrathin Bi(110) and Bi(111) films. Bi(111) films were observed to be kinetically limited at low temperatures. Here, we observe solely the growth of Bi(110) at low temperatures, transforming to Bi(111) around about 400 K. Surprisingly, the Bi(110) (domains) can be grown up to thicknesses of 14 nm, well beyond the critical thickness reported by both, Nagao [24, 27] and Bobaru [39].

To test the hypothesis of Bi(110) and Bi(111) domain competition versus stacking, we study films grown around the transition temperature. In figure 3(b) we show the growth of a 16 nm thick film grown at RT where we measured a (00) CTR at several different thicknesses. The very thin 4 nm Bi film reveals a Bragg reflection for Bi(110) at $L = 4$, but upon increasing the film thickness, the Bragg reflection for Bi(111) at $L = 3.3$ starts developing, and for thicker films the ratio between both peaks becomes more similar. Note that the center of the Bi(110) peak for the 4 nm thick film grown at

RT, is slightly shifted towards higher L as compared to thicker films. This peak position corresponds to a slightly compressed average interlayer distance of 3.24 Å as compared to the bulk interlayer distance of 3.27 Å [1, 58]. From a quantitative low energy electron diffraction (LEED) analysis described in literature [58], contracted interlayer relaxations are present within the first 4 layers of Bi(110), which can heavily contribute to the average interlayer spacing on films of only several double bilayers as is the case here. Although one might anticipate that at RT the Bi(110) film only grows up to a certain thickness and then simply transforms into a Bi(111) film, this cannot be concluded from the increasing area of the peak at $L = 4$ with increasing thickness. This reveals that the Bi(110) film continues to grow up to a significant thickness, indicative of the competition between domains [39].

Realspace *in situ* scanning probe microscopy images might help to study this initial thin film growth around the transition temperature.

4. Conclusions

In summary, we have presented SXRD, CTR and XRR measurements demonstrating the controlled growth of Bi(110) and Bi(111) on an atomically well defined insulating α -Al₂O₃(0001) substrate. At temperatures as low as 40 K, the kinetics of the film growth can be slowed down, resulting in high quality pseudo-cubic Bi(110) films, having rotationally disordered domains and growing solely Bi(110) up to unanticipated thicknesses of tens of nanometers. Bringing the film to RT decreases the film–vacuum and film–substrate roughness, indicative of (electronic) decoupling of the film from the substrate. By heating the Bi(110) film above 400 K a crystallographic orientation transition occurs to Bi(111).

High quality and ultrasoft Bi(111) films can be produced by heating Bi(110) to 450 K onwards, where the roughness of the film–vacuum interface is below 1 Å and the roughness between film and substrate decreases with increasing temperature. The films show a slight preferential alignment with respect to the substrate.

At temperatures around the crystallographic orientation transition (\approx 400 K), the growth of Bi(110) and Bi(111) domains are in competition. A film grown at this temperature results in the growth of thin Bi(110) domains followed by thicker Bi(111) domains.

The growth of Bi(110) structures on α -Al₂O₃(0001) is unanticipated but will have interesting electronic properties [1, 2, 10]. The growth and possible coexistence of both Bi(110) and Bi(111) films on an insulating substrate is very attractive for future electronic and practical applications, as the interface between substrate and film, expected to reveal topological states, will be protected from influencing oxidation effects upon ambient exposure [19]. The electronic properties of the buried interface could, e.g., be probed by second-order nonlinear optical spectroscopy [59]. The lateral disorder in these films and accompanying compressive and

tensile strain in the vicinity of grain boundaries, might easily enhance or destroy surface states [60].

Acknowledgments

MJ and TRJB would like to thank Helena Isern and Thomas Dufrane for their technical assistance. This work is part of the research programme of the Foundation for Fundamental Research on Matter (FOM), which is part of the Netherlands Organisation for Scientific Research (NWO). TRJB acknowledges ESRF beamtime granted for this study under proposal no MA-2475.

References

- [1] Hofmann P 2006 The surface of bismuth: structural and electronic properties *Prog. Surf. Sci.* **81** 191–245
- [2] Koroteev Y M, Bihlmayer G, Chulkov E V and Blügel S 2008 First-principles investigation of structural and electronic properties of ultrathin Bi films *Phys. Rev. B* **77** 045428
- [3] Xiao S, Wei D and Jin X 2012 Bi(111) thin film with insulating interior but metallic surfaces *Phys. Rev. Lett.* **109** 166805
- [4] Yang F *et al* 2012 Spatial and energy distribution of topological edge states in single Bi(111) bilayer *Phys. Rev. Lett.* **109** 016801
- [5] Ando Y 2013 Topological insulator materials *J. Phys. Soc. Japan* **82** 102001
- [6] Sabater C, Gosálbez-Martnez D, Fernández-Rossier J, Rodrigo J G, Untiedt C and Palacios J J 2013 Topologically protected quantum transport in locally exfoliated bismuth at room temperature *Phys. Rev. Lett.* **110** 176802
- [7] Aitani M, Hirahara T, Ichinokura S, Hanaduka M, Shin D and Hasegawa S 2014 *In situ* magnetotransport measurements in ultrathin Bi films: evidence for surface-bulk coherent transport *Phys. Rev. Lett.* **113** 206802
- [8] Drozdov I K, Alexandradinata A, Jeon S, Nadj-Perge S, Ji H, Cava R J, Bernevig A and Yazdani A 2014 One-dimensional topological edge states of bismuth bilayers *Nat. Phys.* **10** 664–9
- [9] Aguilera I, Friedrich C and Blügel S 2015 Electronic phase transitions of bismuth under strain from relativistic self-consistent *gw* calculations *Phys. Rev. B* **91** 125129
- [10] Miao L *et al* 2015 Evolution of the electronic structure in ultrathin Bi(111) films *Phys. Rev. B* **91** 205414
- [11] Du H *et al* 2016 Surface Landau levels and spin states in bismuth (111) ultrathin films *Nat. Commun.* **7** 10814
- [12] Reis F, Li G, Dudy L, Bauernfeind M, Glass S, Hanke W, Thomale R, Schäfer J and Claessen R 2016 Bismuthene on a SiC substrate: a candidate for a new high-temperature quantum spin Hall paradigm arXiv:1608.00812 <https://arxiv.org/abs/1608.00812>
- [13] Song F, Wells J W, Jiang Z, Saxegaard M and Wahlström E 2015 Low-temperature growth of bismuth thin films with (111) facet on highly oriented pyrolytic graphite *ACS Appl. Mater. Interfaces* **7** 8525–32
- [14] Lu Y *et al* 2015 Topological properties determined by atomic buckling in self-assembled ultrathin Bi(110) *Nano Lett.* **15** 80–7
- [15] Yao M-Y, Zhu F, Han C Q, Guan D D, Liu C, Qian D and Jia J-F 2016 Topologically nontrivial bismuth(111) thin films *Sci. Rep.* **6** 21326
- [16] Bian G, Wang Z, Wang X-X, Xu C, Xy S Y, Miller T, Hasan M Z, Liu F and Chang Chiang T 2016 Engineering

- electronic structure of a two-dimensional topological insulator Bi(111) bilayer on Sb nanofilm by quantum confinement effect *ACS Nano* **10** 3859
- [17] Liu Z, Liu C-X, Wu Y-S, Duan W-H, Liu F and Wu J 2011 Stable nontrivial Z_2 topology in ultrathin Bi (111) films: a first-principles study *Phys. Rev. Lett.* **107** 136805
- [18] Lima E N and Schmidt T M 2015 Topological phase driven by confinement effects in Bi bilayers *Phys. Rev. B* **91** 075432
- [19] Tabor P, Keenan C, Urazhdin S and Lederman D 2011 Molecular beam epitaxy and characterization of thin Bi₂Se₃ films on Al₂O₃(110) *Appl. Phys. Lett.* **99** 013111
- [20] Walker E S et al 2016 Large-area dry transfer of single-crystalline epitaxial bismuth thin films *Nano Lett.* **16** 6931–8
- [21] Tanaka A, Hatano M, Takahashi K, Sasaki H, Suzuki S and Sato S 1999 Growth and angle-resolved photoemission studies of bismuth epitaxial films *Surf. Sci.* **433-435** 647–51
- [22] Nagao T, Doi T, Sekiguchi T and Hasegawa S 2000 Epitaxial growth of single-crystal ultrathin films of bismuth on Si(111) *Japan. J. Appl. Phys.* **39** 4567–70
- [23] Yaginuma S, Nagao T, Sadowski J T, Pucci A, Fujikawa Y and Sakurai T 2003 Surface pre-melting and surface flattening of Bi nanofilms on Si(111)-7 × 7 *Surf. Sci.* **547** L877–81
- [24] Nagao T, Sadowski J T, Saito M, Yaginuma S, Fujikawa Y, Kogure T, Ohno T, Hasegawa Y, Hasegawa S and Sakurai T 2004 Nanofilm allotrope and phase transformation of ultrathin Bi film on Si(111)-7 × 7 *Phys. Rev. Lett.* **93** 105501
- [25] Kammler M and von Hoegen M H 2005 Low energy electron diffraction of epitaxial growth of bismuth on Si(111) *Surf. Sci.* **576** 56–60
- [26] Mönig H, Sun J, Koroteev Y M, Bihlmayer G, Wells J, Chulkov E V, Pohl K and Hofmann P 2005 Structure of the (111) surface of bismuth: LEED analysis and first-principles calculations *Phys. Rev. B* **72** 085401
- [27] Nagao T, Yaginuma S, Saito M, Kogure T, Sadowski J T, Ohno T, Hasegawa S and Sakurai T 2005 Strong lateral growth and crystallization via two-dimensional allotropic transformation of semi-metal Bi film *Surf. Sci.* **590** 247–52
- [28] Yaginuma S, Nagao T, Sadowski J T, Saito M, Nagaoka K, Fujikawa Y, Sakurai T and Nakayama T 2007 Origin of flat morphology and high crystallinity of ultrathin bismuth films *Surf. Sci.* **601** 3593–600
- [29] Lükermann D, Banyoudeh S, Brand C, Sologub S, Pfnür H and Tegenkamp C 2014 Growth of epitaxial Bi-films on vicinal Si(111) *Surf. Sci.* **621** 82–7
- [30] Kokubo I, Yoshiike Y, Nakatsuji K and Hirayama H 2015 Ultrathin Bi(110) films on Si(111) 3 × 3-b substrates *Phys. Rev. B* **91** 075429
- [31] Scott S A, Kral M V and Brown S A 2005 A crystallographic orientation transition and early stage growth characteristics of thin Bi films on HOPG *Surf. Sci.* **587** 175–84
- [32] McCarthy D N, Robertson D, Kowalczyk P J and Brown S A 2010 The effects of annealing and growth temperature on the morphologies of Bi nanostructures on HOPG *Surf. Sci.* **604** 1273–82
- [33] Kowalczyk P J, Mahapatra O, McCarthy D N, Kozlowski W, Klusek Z and Brown S A 2011 STM and XPS investigations of bismuth islands on HOPG *Surf. Sci.* **605** 659–67
- [34] Jeffrey C A, Zheng S H, Bohannon E, Harrington D A and Morin S 2006 x-ray characterization of as-deposited, epitaxial films of Bi(012) on Au(111) *Surf. Sci.* **600** 95–105
- [35] Kim D-H, Lee S-H, Kim J-K and Lee G-H 2006 Structure and electrical transport properties of bismuth thin films prepared by RF magnetron sputtering *Appl. Surf. Sci.* **252** 3525–31
- [36] Hattab H, Zubkov E, Bernhart A, Jnawali G, Bobisch C, Krenzer B, Acet M, Möller R and Horn von Hoegen M 2008 Epitaxial Bi(111) films on Si(001): strain state, surface morphology, and defect structure *Thin Solid Films* **516** 8227–31
- [37] Payer T, Rajkovic I, Ligges M, von der Linde D, von Hoegen M H and zu Heringdorf F-J M 2008 Ultrathin epitaxially grown bismuth (111) membranes *Appl. Phys. Lett.* **93** 093102
- [38] Zhang H L, Chen W, Wang X S, Yuhara J and Wee A T S 2009 Growth of well-aligned Bi nanowire on Ag(111) *Appl. Surf. Sci.* **256** 460–4
- [39] Bobaru S, Gaudry É, de Weerd M-C, Ledieu J and Fournée V 2012 Competing allotropes of Bi deposited on the Al₁₃Co₄ (100) alloy surface *Phys. Rev. B* **86** 214201
- [40] Bui T N, Raskin J-P and Hackens B 2016 Semiconductor-to-metallic-like behavior in Bi thin films on KCl substrate *J. Appl. Phys.* **119** 135304
- [41] Campbell C T 1997 Ultrathin metal films and particles on oxide surfaces: structural, electronic and chemisorptive properties *Surf. Sci. Rep.* **27** 1–111
- [42] Ernst K H, Ludviksson A, Zhang R, Yoshihara J and Campbell C T 1993 Growth model for metal films on oxide surfaces: Cu on ZnO(0001)-O *Phys. Rev. B* **47** 13782–96
- [43] Campbell C T 1994 Model for the growth and reactivity of metal films on oxide surfaces: Cu on ZnO(0001) *J. Vac. Sci. Technol. A* **12** 1825
- [44] Rosenfeld G, Servaty R, Teichert C, Poelsema B and Comsa G 1993 Layer-by-layer growth of Ag on Ag(111) induced by enhanced nucleation: a model study for surfactant-mediated growth *Phys. Rev. Lett.* **71** 895–8
- [45] Zhang Z 1997 Atomistic processes in the early stages of thin-film growth *Science* **276** 377–83
- [46] Wu K S and Chern M Y 2008 Electrical transport properties of n-type (110)-oriented bismuth thin films grown at 110 k on glass substrates *J. Appl. Phys.* **104** 033704
- [47] Balmes O, van Rijn R, Wermeille D, Resta A, Petit L, Isern H, Dufrane T and Felici R 2009 The {ID03} surface diffraction beamline for *in situ* and real-time x-ray investigations of catalytic reactions at surfaces *Catal. Today* **145** 226
- [48] Okamoto H 1991 *Binary Alloy Phase Diagrams* (Metals Park: ASM International)
- [49] Ponchut C, Rigal J M, Clément J, Papillon E, Homs A and Petitdémange S 2011 Maxipix, a fast readout photon-counting x-ray area detector for synchrotron applications *J. Instrum.* **6** C01069
- [50] Roobol S, Onderwaater W, Drnec J, Felici R and Frenken J 2015 Binoculars: data reduction and analysis software for two-dimensional detectors in surface x-ray diffraction *J. Appl. Crystallogr.* **48** 1324–9
- [51] Björck M and Andersson G 2007 GenX: an extensible x-ray reflectivity refinement program utilizing differential evolution *J. Appl. Crystallogr.* **40** 1174–8
- [52] Patterson A L 1939 The Scherrer formula for x-ray particle size determination *Phys. Rev.* **56** 978–82
- [53] Takagi M 1954 Electron-diffraction study of liquid–solid transition of thin metal films *J. Phys. Soc. Japan* **9** 359–63
- [54] Vlieg E 2012 *Surface and Interface Science, Vols 1 and 2: Vol 1—Concepts and Methods* (New York: Wiley)
- [55] Henry C R, Chapon C, Duriez C and Giorgio S 1991 Growth and morphology of palladium particles epitaxially deposited on a MgO(100) surface *Surf. Sci.* **253** 177–89
- [56] Bäumer M, Libuda J, Sandell A, Freund H-J, Graw G, Bertrams Th and Neddermeyer H 1995 The growth and properties of Pd and Pt on Al₂O₃/NiAl(110) *Ber. Bunsenges. Phys. Chem.* **99** 1381–6
- [57] Zhang T C, Mei Z X, Guo Y, Xue Q K and Du X L 2009 Influence of growth temperature on formation of continuous Ag thin film on ZnO surface by ultra-high vacuum deposition *J. Phys. D: Appl. Phys.* **42** 065303
- [58] Sun J, Mikkelsen A, Fuglsang Jensen M, Koroteev Y M, Bihlmayer G, Chulkov E V, Adams D L, Hofmann P and Pohl K 2006 Structural determination of the Bi(110)

- semimetal surface by leed analysis and *ab initio* calculations
Phys. Rev. B **74** 245406
- [59] Hsieh D, McIver J W, Torchinsky D H, Gardner D R,
Lee Y S and Gedik N 2011 Nonlinear optical probe of
tunable surface electrons on a topological insulator *Phys.*
Rev. Lett. **106** 057401
- [60] Liu Y, Li Y Y, Rajput S, Gilks D, Lari L, Galindo P L,
Weinert M, Lazarov V K and Li L 2014 Tuning Dirac states
by strain in the topological insulator Bi₂Se₃ *Nat. Phys.* **10**
294–9